THAP7-AS1 recruits the SWI/SNF to activate EGFR-ELK1 signaling and induce crosstalk between tumor-associated macrophages and breast cancer cells

Hai-Ting Liu
Shandong University
Zhao-Xin Gao
Shandong University
Guo-Hao zhang
Shandong University
Xiang-Yu Guo
Shandong University
Xing-Chen Zhou
Second Hospital of Shandong University
Rui-Nan Zhao
Shandong University
Sen Liu
Shandong University
Wen-Jie Zhu
Shandong University
Feng-Zhen Zhang
Second Hospital of Shandong University
Han Wang
Shandong University
Chuan-Zong Zhao
Shandong University
Xiao Wang
Shandong University
Peng Gao (gaopeng@sdu.edu.cn)
Shandong University

Research Article

Keywords: TAM, IL-10, THAP7-AS1, SWI/SNF complex, EGFR

Posted Date: March 17th, 2022

DOI: https://doi.org/10.21203/rs.3.rs-1453689/v1

Abstract

Background

Accumulating evidence indicates that the crosstalk between tumor cells and the microenvironment influences human cancer progression. However, the expression pattern, function role in the crosstalk between tumor cells and tumor microenvironment, and underlying mechanism of lncRNAs-related tumorigenesis in breast cancer are unknown.

Methods

The expression lncRNA-THAP7-AS1 in breast cancer (BC) were identified by in BC tissues. The functional roles of THAP7-AS1 were confirmed by *in vitro* and *in vivo* experiments. RNA-pulldown followed by mass spectrometry, RNA Immunoprecipitation (RIP), chromatin immunoprecipitation (ChIP) assays and luciferase reporter assay revealed the mechanisms of THAP7-AS1 in BC. RT-qPCR, ELISA assays, Flow cytometry, ChIP assays and luciferase reporter assay elucidated the crosstalk between tumor cells and (tumor-associated macrophages) TAMs.

Results

Here, we demonstrate that long non-coding RNA (lncRNA) THAP7-AS1 induces polarization of macrophages to the M2 phenotype in an IL-4-dependent manner, and M2 tumor-associated macrophages (TAMs) secreted IL-10, which then facilitates the progression of breast cancer (BC). Mechanistically, THAP7-AS1 promoted the combination between SNF2H, SNF2L, and BAF155 and recruited the SWI/SNF complex to the promoter of EGFR to upregulate its expression, and then induced IL-4-mediated M2 polarization of macrophages via activation of the EGFR-ELK1 signaling. Reciprocally, IL-10 released from M2 TAMs upregulates CEBP-β-dependent P300 expression, and then P300, synergistically worked with c-MYC and upregulated THAP7-AS1 expression in BC cells, which constituting a feed-forward loop between tumor cells and TAMs. Moreover, THAP7-AS1 knockdown inhibits the invasion, metastasis and M2 macrophage polarization of breast cancer *in vivo*.

Conclusions

Our study highlights the role of THAP7-AS1 in the regulation crosstalk between TAM and tumor cells in BC progression and may provide a novel therapeutic target for BC treatment.

Introduction

Breast cancer (BC) is the most leading cause of cancer-related deaths in women and its burden is increasing worldwide (1). Currently, cancer treatment is becoming much more personalized and

molecularly targeted (2). Despite continuous efforts to improve the overall survival and prognosis of BC patients in recent years, management of patients with metastatic BC remains a huge challenge (3). Thus, it is important to elucidate the specific target and identify the potential mechanism of BC metastasis, which is also critical for the development of novel therapeutic strategies and in improving the survival rate for BC patients.

Many studies have revealed that the spread of cancer is remarkably relevant to their tumor microenvironment (TME), which comprises tumor-associated macrophages (TAMs), blood vessels, stromal cells and extracellular matrix components (4). TAMs are major components of the TME. A growing number of studies have indicated that TAMs can secrete significant amounts of cytokines, including chemokines, inflammatory factors, and growth factors that are involved in the regulation of tumor invasion and metastasis (5). Moreover, evidence from most of these investigations has suggested that TAM density is strongly associated with poor prognosis in several types of cancer, including BC (6, 7). TAMs display two main phenotypes, namely pro-inflammatory (M1) and anti-inflammatory (M2), which usually have distinct effects on tumor progression and metastasis. Tumor cells can release a variety of cytokines to induce the polarization of TAMs (8). Macrophage differentiation such as the M1 or M2 phenotypes is modulated by a series of microenvironmental signals that originate from tumor cells.

Long non-coding RNAs (lncRNAs) are a heterogeneous class of transcripts that are longer than 200 nt and have limited protein-coding potential (9). Emerging evidence has implicated that lncRNAs are involved in a wide range of biological processes in human cancers (10–12). However, the roles of lncRNAs in the crosstalk between tumor cells and the tumor microenvironment remain unclear.

LncRNA THAP7-AS1 is a natural antisense lncRNA that is located on chromosome 22q11.21. Our previous study showed that THAP7-AS1 ranks as one of the most significantly upregulated lncRNAs in human gastric cancer (GC) tissues by lncRNA microarray screening and tissue sample validation (GSE72307). However, the expression pattern, function role in the crosstalk between tumor cells and tumor microenvironment, and underlying mechanism of THAP7-AS1-related tumorigenesis in BC are unknown.

In the present study, we discovered that THAP7-AS1, which was significantly upregulated in BC tissues, plays an oncogenic lncRNA that is involved in BC development and progression. THAP7-AS1 recruits the SWI/SNF complex to trigger EGFR expression, and then activates EGFR-ELK1 signaling to promote BC metastasis, which results in the polarization of TAMs towards the M2 phenotype by promoting ELK1-mediated IL-4 expression in BC. Importantly, IL-10 secreted by TAMs may activate the CEBP-β-induced P300 expression. In addition, P300, which cooperates with the transcription factor (TF) c-MYC, could activate THAP7-AS1 transcription to form a positive feedback loop to maintain BC progression. Our findings highlight a crosstalk between TAMs and tumor cells to continuously initiate overexpression of THAP7-AS1 in BC.

Methods

Tissue samples

A total of 44 fresh BC tissues and 8 nontumorous breast tissues were collected from the Qilu Hospital of Shandong University (Shandong Province, China). All patients signed an informed consent form before the study, which was approved by the Research Ethics Committee of Shandong University (Approval No: 201301015).

Cell culture and transfection

Human nontumorous mammary epithelial cells MCF10A, human breast cancer (BC) cell lines MDA-MB-231, MDA-MB-468, MCF-7, and T47D, human embryonic kidney 293T cells and THP-1 monocytes were purchased from American Type Culture Collection (ATCC) and were cultured under conditions specified in the cell culture manual. For transient transfection, MDA-MB-231 and MDA-MB-468 cells were transfected with plasmid or siRNA using Tuberfect and Lipofectamine 2000 (Thermo Fisher Scientific, USA) according to the manufacturer's instructions. The sequences of the siRNAs are shown in Supplementary Table 1-2. For stable transfection, MDA-MB-231 and MDA-MB-468 cells stably transfected with LV5-THAP7-AS1 or LV5-NC and LV3-sh-THAP7-AS1 or LV3-sh-NC (GenePharma, Shanghai, China) were grown in 1 μg/mL puromycin (Invitrogen).

RNA isolation and RT-qPCR

Total RNA from BC tissues, nontumorous breast tissues, and cancer cells was isolated using TRIzol reagent (Invitrogen, Carlsbad, CA, USA). RNA from the cytoplasmic and nuclear fractions of the BC cells was prepared with NE-PER Nuclear and Cytoplasmic Extraction Reagents (Thermo Scientific, Waltham, MA, USA) according to the manufacturer's protocol. RNA was reverse-transcribed, and qPCR was performed for determining RNA expression levels.

Western blotting analysis

Cells were harvested and lysed on ice in RIPA buffer with protease and phosphatase inhibitors, and proteins were extracted. Western blotting was performed as previously described, with antibodies specific to SNF2H (Abcam), SNF2L (Abcam), BAF155 (Abcam), EGFR (Proteintech), RRAS (Proteintech), B-RAF (Proteintech), p-BRAF (Abcam), C-RAF (Proteintech), p-CRAF (Abcam), MEK (Proteintech), p-MEK (CST), MAPK (Proteintech), p-MAPK (CST), ELK1 (Proteintech), P300 (Santa Cruz), GAPDH (Abways) and β-actin (Abways).

RNA-Seq analysis

RNA-seq of SI-THAP7-AS1-or SI-NC-transfected MDA-MB 231 and MDA-MB-468 cells was conducted using Solexa pipeline v1.8 (Off-Line Base Caller software, v1.8, Illumina, Foster City, CA, USA). Genes that were commonly downregulated (by^3 1.5-fold) in the Si-THAP7-AS1 group, compared with the si-NC group, were selected for further analysis. Gene set enrichment analysis (GSEA) was conducted using GSEA. Differentially expressed genes were identified by comparing each pair (Si-THAP7-AS1 vs. Si-NC). The raw

data can be accessed via NCBI's Gene Expression Omnibus as accession numbers GSE 150539 and GSE 160685.

Fluorescence in situ hybridization and immunofluorescence analysis

THAP7-AS1 fluorescence in situ hybridization (FISH) probe was synthesized by Ribo BioTechnology Co., Ltd. (Guangzhou, China). RNA FISH was performed with the FISH kit to detect the subcellular localization of THAP7-AS1 in BCs according to the manufacturer's protocol (Ribo Bio Tech). The protein expression levels of SNF2H, SNF2L, and BAF155 in both BC cells were determined by immunofluorescence with anti-SNF2H (Santa Cruz), anti-SNF2H (Affinity), and anti-SNF2H (Santa Cruz) antibodies.

Cell migration and invasion assays

To measure cell migration and invasion, cells were suspended in 200 μL of serum-free L-15 and seeded into the top chamber uncoated or coated with Matrigel (BD Biosciences) of 24-well plate-sized Transwell inserts (Corning Falcon). After incubation for 16 h, the inserts were fixed, stained, and observed.

Chromatin immunoprecipitation (ChIP) assay

ChIP analysis was performed using a Millipore EZ-ChIP kit (#17–371) following the manufacturer's instructions (Millipore, Temecula, CA, USA). After crosslinking, 6 μg of the antibody against P300 (Proteintech), acetyl-histone H3 Lys27 (H3K27Ac, CST), c-MYC (Proteintech), c-JUN (Santa Cruz), SNF2H (Abcam), SNF2L (Abcam), BAF155(Abcam), and CEBP-β (Santa Cruz), or normal IgG (Millipore) was added to immunoprecipitate endogenous THAP7-AS1 or endogenous EGFR. The precipitated chromatin DNA was analyzed by qPCR. The ChIP primer sequences are listed in Supplementary Table 3-4.

Co-immunoprecipitation (CO-IP) assay

Briefly, protein A/G Sepharose beads were added to the cell lysates and incubated with 4 μg antibody overnight at 4°C. Subsequently, generated immunocomplexes were washed with PBS 10 times and analyzed by western blot.

RNA pull-down assay

RNA pull-down followed by mass spectrometry analysis and in vitro RNA-protein binding assay was performed as previously described (*13*). Biotin-labeled full-length THAP7-AS1 and antisense THAP7-AS1 were synthesized in vitro using T7 RNA polymerase in vitro (Ambio Life). The biotinylated RNAs were mixed and incubated with MDA-MB-468 cell lysates. After elution of THAP7-AS1-interacting proteins, these were resolved by SDS-PAGE followed by silver staining and subjected to mass spectrometric analysis.

RNA immunoprecipitation (RIP) assay

RIP experiments were performed using the Megna RIP RNA-binding protein immunoprecipitation kit (Millipore) according to the manual. Anti-SNF2H, anti-SNF2L, and anti-BAF155 antibodies used for RIP were purchased from Abcam. The co-precipitated RNAs were detected by RT-qPCR.

Construction of vectors

Full-length THAP7-AS1 cDNA was cloned into the pCDNA3.1 expression vector and synthesized by Invitrogen (Beauchamp Biology Co. Ltd., Shanghai, China). SNF2H, SNF2L, and BAF155 vectors were purchased from Vigene Biosciences (Rockville, MD, USA). pcDNA3.1-P300 was a gift from Warner Greene (Addgene plasmid # 23252; http://n2t.net/addgene:23252). pcDNA3.1-c-MYC, pcDNA3.1-KLF5, pcDNA3.1-ELK1, pcDNA3.1-CREB, pcDNA3.1-c-JUN, PENTER-c-MYB, PENTER-YY1, and PENTER-CEBP-β were generated in our previous study. Luciferase reporter vector, including pGL3-P300-2,000/0, pGL3-EGFR-2,012/0, pGL3-EGFR-1,512/0, pGL3-EGFR-1,012/0, and pGL3-EGFR-512/0 was synthesized by Invitrogen (Beauchamp Biology Co, Ltd., Shanghai, China). PGL3-THAP7-AS1 luciferase reporter vectors (PGL3-2,000/0, PGL3-509/0, PGL3-210/0, PGL3-155/0, and PGL3-101/0) were generated in our previous study.

Luciferase reporter assay

THAP7-AS1 promoter, EGFR promoter region and serial truncations promoter region, and P300 promoter region were synthesized and cloned into a pGL3-basic vector. The putative transcription factor (TF)-binding motif in the promoter region of THAP7-AS1 was identified using ALGGEN program (http://alggen.lsi.upc.edu/). All vectors were confirmed by sequencing, and firefly and Renilla luciferase activities were measured using the Dual Luciferase Assay Kit (Promega) following the manufacturers' protocol.

Enzyme-linked immunosorbent assay (ELISA)

ELISA was performed in accordance with the supplier's instructions. IL-4 (human) and IL-10 (human) levels in the culture supernatant of treated cells were detected using a kit [Multi Sciences (Lianke) Biotech Co., Ltd.].

Flow cytometry

The THP-1 monocytes were harvested and cell suspension were washed with cold PBS. The cells were then stained with CD206-PE (human) antibodies (BioLegend, USA). The cells were examined using a BD flow Cytometer (BD Biosciences, Germany).

Immunohistochemistry (IHC)

IHC staining was conducted as previously described. Paraffin-embedded xenograft tumor tissues from nude mice were stained with CD-163. The score for CD-163 staining was semi-quantitatively evaluated as previously reported (*14*).

In vivo assay

Four-week-old female athymic BALB/c nude mice were purchased from the National Laboratory Animal Center (Weitonglihua Biotechnology, Beijing, China) and maintained under SPF room conditions in accordance with the institutional guidelines for animal care. LV-sh-THAP7-AS1- or empty vector-stably transfected MDA-MB-231 cells were harvested. For subcutaneous injection models, 1×10^8 MDA-MB-231 cells in 150 μL of sterile PBS were inoculated subcutaneously into the axillary fossa mammary fat pads of mice (n = 5 in each group). In assays to measure formation of lung metastases, 1×10^6 MDA-MB-231 cells were injected into the lateral tail vein of mice. Tumors were measured by caliper once a week. Half of the xenografts, lungs, kidneys, and liver were excised, formalin-fixed, and paraffin-embedded, followed by hematoxylin and eosin (H and E) staining. The other half of the xenografts were snap-frozen for subsequent RNA and protein extraction. This study was approved by the Ethical Committee of Shandong University, China (Approval No: 2012028).

Statistical analysis

All statistical analyses were performed using Prism GraphPad 5.0. All quantitative data are presented as the mean ± standard deviation (SD), and $P < 0.05$ was considered statistically significant. Differences between two or multiple groups were evaluated using a student's t-test. Chi-squared test was used to analyze the correlation between THAP7-AS1 expression and clinicopathological parameters. Spearman's rank correlation coefficient was performed to determine the correlation between P300 and THAP7-AS1, THAP7-AS1, and EGFR.

Results

THAP7-AS1 is upregulated in human BC tissues and enhances BC cell metastatic ability

In our previous study, THAP7-AS1 was identified as a novel lncRNA that promotes GC progression by differential expression profiles of lncRNA (GSE72307). To explore the relevance of THAP7-AS1 in human BC, we investigated THAP7-AS1 expression in a cohort of 44 BC tumors and 8 non-tumor breast tissues. The results showed that THAP7-AS1 expression was significantly higher in the tumor tissues than that of in non-tumor breast tissues, and further increased in lymph node metastatic BC compared with those without metastasis (Figures 1A-B). A receiver operating characteristic (ROC) curve was performed to evaluate whether THAP7-AS1 expression could be used to distinguish patients with or without LNM. The area under the curve (AUC) value for THAP7-AS1, which was constructed to distinguish BC cases with and without LNM, reached up to 0.7346 (Figure 1C). Moreover, analyses of The Cancer Genome Atlas (TCGA) database indicated that THAP7-AS1 was expressed at higher levels in various types of human cancer, such as adrenocortical, AML, esophageal, liver, lung, and pancreatic cancer (Supplementary Figures 1A-F), and THAP7-AS1 overexpression was associated with poor prognosis in human cancers, including lung cancer and GC (Supplementary Figures 1G-H), which further suggests that THAP7-AS1 plays an oncogenic role in progression and development of various human cancers. We further examined

THAP7-AS1 expression levels in a panel of human BC cell lines. BC cell lines expressed remarkably higher levels of THAP7-AS1 than that of the nontumorous mammary epithelial cell line MCF10A (Figure 1D).

To further study the function of THAP7-AS1, we used Smart Silencer targeting THAP7-AS1 and control. As shown in Figures 1E-H, PcDNA3.1-THAP7-AS1 -mediated overexpression and the Smart Silencer mediated knockdown were used for exogenously guiding the expression of THAP7-AS1 in MDA-MB-231 and MDA-MB-468 cells. Then, Transwell migration and invasion assays showed that THAP7-AS1 overexpression enhanced cell migration and invasion abilities compared with the control in both BC cells (Figures 1I-J). By contrast, knockdown of THAP7-AS1 effectively suppressed cell migration and invasion (Figures 1K-L). Consistent with these findings, less local infiltration and metastatic colonies in the lungs were observed in xenograft tumor models of nude mice using MDA-MB-231 cells that were stably transfected with LV3-sh-THAP7-AS1 (Figures 1M-O). In addition, the number of metastatic nodules decreased in nude mice subjected to tail vein administration of ectopic knockdown of THAP7-AS1 compared with the control group. This difference was further verified following examination of H and E staining of lung sections (Figure 1P). Taken together, these findings suggest that THAP7-AS1 promotes BC metastasis and progression.

THAP7-AS1 activates the EGFR signaling pathway

To investigate the molecular mechanism of THAP7-AS1 in promoting BC metastasis, first, we investigated whether THAP7-AS1 functions *in cis*, affecting the expression of nearby gene (THAP7; THAP7-AS1 is an antisense transcript of THAP7). However, the overexpression and knockdown of THAP7-AS1 did not affect the expression of THAP7 (Figures 2A-D), indicating that it did not exert its function its function *in cis*. Then, RNA subcellular fractionation location and FISH assays demonstrated that THAP7-AS1 is mainly localized in the nucleus (Figures 2E-J), thus suggesting that THAP7-AS1 binds to nuclear nucleus molecules or proteins and transcriptionally regulate gene functions. To explore changes in the expression of genes downstream of THAP7-AS1, we established the global effects of THAP7-AS1- silenced MDA-MB-231 and MDA-MB-468 cells and conducted RNA transcriptome sequencing. THAP7-AS1 knockdown, respectively, affected the expression of 1,349 genes (585 downregulated and 764 upregulated) and 725 genes (318 downregulated and 407 upregulated) in MDA-MB-231 cells and MDA-MB-468 cells (Supplementary Figures 2A-B). KEGG pathway analysis and GSEA revealed that THAP7-AS1 regulates many genes that are associated with cancer-related signaling processes, including the ERBB (EGFR) signaling pathway (Supplementary Figures 2C-D and Figure 2K). Remarkably, western blotting assays showed that THAP7-AS1 overexpression significantly upregulated the expression of some major EGFR signaling targets, including EGFR, RRAS, and ELK1 and phosphorylation of BRAF, CRAF, MAPK, and ERK in both BC cells (Figure 2L). However, the expression of BRAF, CRAF, MAPK and ERK did not show a significant difference between the groups. By contrast, THAP7-AS1 depletion reduced the expression of EGFR and major EGFR targets (Figures 2M-N). These data indicate that THAP7-AS1 activates the EGFR signaling pathway in BC. Next, we explored the expression levels of THAP7-AS1 and EGFR in BC tissues by RT-qPCR. We noticed that THAP7-AS1 expression was positively associated with EGFR expression ($r = 0.2883$, $p = 0.0382$) (Figure 2O). In

summary, THAP7-AS1 initiates EGFR expression to activate the EGFR signaling pathway, leading to tumor progression.

THAP7-AS1 directly binds to SWI/SNF Complex

LncRNAs could exert their functions by interacting with RNA binding proteins that regulate the expression of target genes by various mechanisms (*15*). Therefore, RNA pull-down assay followed by proteomic analysis of the THAP7-AS1-combined protein complex in MDA-MB-468 cells was performed to search for potential THAP7-AS1-related proteins (Figure 3A). SNF2H, SNF2L, and BAF155, three core subunits of the SWI/SNF complex, were selected for further binding confirmation based on the following criteria: (1) molecular weight of approximately 130 kD; (2) peptide score > 300; (3) subcellular localization in the nucleus; and (4) reportedly relates to tumor progression. RNA pull-down and RNA immunoprecipitation was further confirmed the interaction between the three SWI/SNF components and THAP7-AS1 (Figures 3B-H). Moreover, THAP7-AS1 colocalized with SNF2H (Figure 3I), SNF2L (Figure 3J) and BAF155 (Figure 3K) in the nuclei of BC cells. These findings indicate that THAP7-AS1 is correlated with the SWI/SNF complex in the nuclei of BC cells. THAP7-AS1 overexpression and depletion did not affect the expression levels of SNF2H, SNF2L and BAF155 (Figures 2L-N), indicating that THAP7-AS1 is not involved in the regulation of the SWI/SNF complex at the post-translational level. However, overexpression of THAP7-AS1 promoted the combination between SNF2H and SNF2L and BAF155 (Figure 3L). Additionally, through domain mapping, we observed that segment 1 (–) of THAP7-AS1 interacted with SNF2H, segment 2 (–) combined with SNF2L, whereas segment 3 (–) bound to BAF155 (Figure 3M). These findings suggest that THAP7-AS1 directly binds to the SWI/SNF complex and promotes interactions among the three proteins.

THAP7-AS1 triggers EGFR expression through recruitment of the SWI/SNF complex to activate EGFR signaling

There is mounting evidence that the SWI/SNF complex regulates gene expression at the transcriptional level by binding to the promoter region and remodeling chromatin(*16*). Hence, we thus explored whether the activation of EGFR signaling by THAP7-AS1 is dependent on the initiation of SNF2H/SNF2L/BAF155 on the EGFR promoter. First, we designed and used primers that were located ~2 kb upstream of the transcription start sites (TSSs) of EGFR (sites EGFR 1-10). ChIP assays with antibodies against SNF2H, SNF2L, and BAF155 or control IgG showed that SNF2H, SNF2L, and BAF155 efficiently immunoprecipitated the promoter regions of EGFR (Figures 4A-B), suggesting that the promoter regions of EGFR could be regulated by the SWI/SNF complex. Then, we investigated the effect of THAP7-AS1 on SNF2H, SNF2L, and BAF155 binding with the promoter region of the EGFR gene. We observed that THAP7-AS1 depletion reduced the binding capacity of SNF2H, SNF2L, and BAF155 with the EGFR promoter (Figures 4C-E). Moreover, the interaction of SNF2H, SNF2L, and BAF155 with the EGFR promoter region can be enhanced by THAP7-AS1 upregulation (Figures 4F-H), indicating that THAP7-AS1 enhanced SNF2H, SNF2L, and BAF155 occupancy of the promoter region of the EGFR. To identify which segment of the EGFR promoter is the core binding site for THAP7-AS1, the promoter activities of a 2,012-bp region

upstream of the TSS (pGL3-2,000/0) and three deletion constructs, including pGL3-1,512/0, pGL3-1,012/0, and pGL3-512/0, were determined in THAP7-AS1 deleted and upregulated BC cells. We found (approximately) the -1,012 to -512 bp segment of EGFR promoter as a sufficient binding site for THAP7-AS1 (Figures 4I-L). Our findings indicate that THAP7-AS1 recruits the SWI/SNF complex to the EGFR promoter, which then results in its activation. Remarkably, SNF2H and SNF2L were highly expressed in BC tumors compared with non-tumorous breast tissues (Figures 4M-N), indicating that the SWI/SNF complex may participate in the regulation of BC progression. Additionally, we analyzed RNA-Seq data [from The Cancer Genome Atlas (TCGA)] of the SWI/SNF complex of BC. Figure 4O shows that BAF155 was remarkably upregulated in BC tissues from the TCGA data. Additionally, SNF2H, SNF2L, and BAF155 deletion notably impaired the migration and invasion ability in both BC cells (Supplementary Figures 3A-D). Next, we found that SNF2H, SNF2L, and BAF155 knockdown dramatically decreased the expression of EGFR (Figures 4P-Q) and the key downstream molecules including RRAS and ELK1, and phosphorylation of BRAF, CRAF, MAPK and ERK (Supplementary Figure 3E). However, there was no difference in EGFR expression between the SNF2H, SNF2L, and BAF155 upregulation group and the control (Figures 4R-S). THAP7-AS1 overexpression and knockdown significantly respectively promoted and inhibited the expression of EGFR (Figures 4T-W). The above results indicated that the SNF/SWI complex regulates the EGFR upregulation depending on the presence of THAP7-AS1. Taken together, our data indicate that THAP7-AS1 triggers EGFR expression through the recruitment of the SWI/SNF complex to the -1,012 to -512 bp segment of the EGFR promoter, resulting in the activation of EGFR-ELK1 signaling.

P300 and c-MYC synergistically activates THAP7-AS1 transcription

To explore upstream regulatory mechanisms of THAP7-AS1 overexpression in BC, epigenetic modification and detailed promoter analysis were performed. First, we treated four kinds of BC cell lines with 5-azacytidine (5-AZ, demethylating agent), trichostatin A (TSA; histone deacetylase inhibitor) and 3-deazaneplanocin A (Dznep, histone methyltransferase EZH2 inhibitor). The results revealed that THAP7-AS1 levels were significantly increased in TSA-treated BC cells (Figure 5A). As we known, TSA influences the expression of genes through induction of histone hyperacetylation at the promoter region (*17*). Our findings indicated that histone acetyltransferase (HAT)/histone deacetylase (HDACs)-mediated histone modification may be one of the epigenetic mechanisms that regulate THAP7-AS1 transcription. Human HATs acetylate lysines, such as PCAF, MORF, HAT11, and P300, leading to a more relaxed, open and transcriptionally active chromatin structure (*18*). The ALGGEN program suggested that there were seven P300-binding sites in the promoter of THAP7-AS1. P300, which possesses intrinsic acetyltransferase activity, belongs to the HAT family and regulates gene transcription via histone acetylation and chromatin remodeling (*19*). To explore whether P300 virtually plays a role in THAP7-AS1 gene transcription activation, a luciferase activity assay was performed. P300 was able to promote the transcriptional activity of the THAP7-AS1 promoter in BC cells (Figures 5B-C). Furthermore, the THAP7-AS1 level increased in BC cells transfected with pcDNA3.1-P300 plasmid relative to the control cells (Figures 5D-E), and was close to the levels in TSA-treated cells. Moreover, the expression of P300, which was high in BC tumors compared with non-tumorous breast tissues (Supplementary Figure 4A), was positively correlated

with THAP7-AS1 levels in BC (Supplementary Figures 4B-C). Next, we used C646, one of the most representative histone acetyltransferase (HAT)-P300 inhibitors, to evaluate the contribution of P300 to THAP7-AS1 expression in BC cells. C646 treatment resulted in a marked reduction in THAP7-AS1 expression in BC cells (Figures 5F-G). In addition, THAP7-AS1 expression decreased after knocking down P300 (Figures 5H-I), close to the level in C646-treated cells. To determine whether P300 interacts with the endogenous THAP7-AS1 promoter, we performed a ChIP assay. Figures 5J-K show that P300 efficiently immunoprecipitated the promoter region of THAP7-AS1 in BC cells. P300 is responsible for the acetylation of H3K27, and elevated H3K27ac levels are a hallmark of active genes (*20, 21*). Thus, the level of active histone acetylation marker H3K27ac was determined. Our results suggested that P300-induced H3K27ac expression was enhanced in the THAP7-AS1 promoter region and was involved in the transcriptional regulation of THAP7-AS1 (Figures 5L-M).

HATs add acetyl groups to lysine residues in the core histone proteins and are associated with euchromatin, a decondensed chromatin structure that allows transcription to proceed and increases gene expression (*18*). To elucidate whether transcription factors regulate THAP7-AS1 expression in BC, the promoter activities of a 2,000-bp region upstream of the TSS (pGL3-2000/0) and deletion constructs, including PGL3-509/0, PGL3-210/0, PGL3-155/0, and PGL3-101/0, were investigated. Our findings showed that the promoter activities of PGL3-210/0 resulted in a 52% decrease in luciferase activity compared to that of pGL3-509/0 (Figures 5N-O), suggesting that the region located between -509 and -210 is the basal promoter of THAP7-AS1. Next, the transcription factor-binding site region from -509 and -210 was analyzed using the ALGGEN program. Five putative binding sites, including that of KLF5, ELK1, c-JUN, CREB, and c-MYC, were determined. To explore their roles in regulating THAP7-AS1 transcription, KLF5, ELK1, c-JUN, CREB, and c-MYC, were, respectively, overexpressed in both BC cells that were transiently transfected with the pGL3-509/0 construct. The results revealed that the promoter activities of pGL3-509/0 remarkably increased in the c-MYC and c-JUN overexpression groups (Figures 5P-Q). Additionally, RT-qPCR assay indicated that c-MYC and c-JUN enhanced the expression of THAP7-AS1(Figures 5R-S). The above results suggest that the c-MYC and c-JUN-binding sites are crucial for THAP7-AS1 transcription. To explore the contribution of the three putative c-JUN-binding sites and the one putative c-MYC-binding site to the regulation of the THAP7-AS1 promoter, we introduced four-point mutations, designated as p (-314 to -320) Luc-c-JUN-1, p (-88 to -94) Luc- c-JUN -2, and p (-15 to -21) Luc-c-JUN -3, and p (-120 to -115) Luc-c-MYC. Luciferase assays showed that the four mutation vectors separately led to a decrease in promoter activity compared with the control in the 293T cells (Figure 5T). Additionally, ChIP assays revealed that positive enrichment of the promoter amplicons of THAP7-AS1 in the c-MYC-binding site and three c-JUN binding sites in BC cells, indicating that c-MYC and c-JUN could directly bind to the promoter of THAP7-AS1 and initiate its transcription (Figures 5U-V and Supplementary Figures 4D-E). To investigate whether c-MYC and c-JUN have a similar synergistic action with P300 on THAP7-AS1 transcription, we co-transfected the PGL3-THAP7-AS1 plasmid and the expression plasmids of P300, c-MYC, and c-JUN into 293T cells, and the results indicated that P300 worked synergistically with c-MYC, rather than c-JUN, to increase promoter activity (Figure 5W). Moreover, P300 and c-MYC synergistically enhanced the expression of THAP7-AS1 in both BC cells (Figure 5X and

Supplementary Figure 4F). These results indicated that P300 synergistically acted with c-MYC to interact with the THAP7-AS1 promoter and increase THAP7-AS1 transcription.

THAP7-AS1 promotes M2 macrophage polarization

We have demonstrated that THAP7-AS1 activates the EGFR-ELK1 signaling pathway. A previous investigation suggested that ELK-1 could bind to the promoter of IL-4 and IL-10 and activate their expression (*22*). To explore the role of THAP7-AS1 in IL-4 and IL-10 expression, RT-qPCR and ELISA assays were performed. The mRNA levels of IL-4 and IL-10 was significantly increased in THAP7-AS1-overexpressed BC cells (Figures 6A-B), and decreased in THAP7-AS1- deleted BC cells (Figures 6C-D), which suggests that IL-4 and IL-10 are positively regulated by THAP7-AS1. We also assessed the cytokine levels in the culture supernatants of THAP7-AS1 ectopically overexpressed and depleted BC cells. Significantly increased IL-4 levels (Figures 6E-F), rather than IL-10 levels (Supplementary Figures 4G-H), were observed in THAP7-AS1 overexpression BC cells, while profoundly decreased IL-4 expression was found in THAP7-AS1-depleted cells (Supplementary Figures 4I-J). IL-4 could polarize TAMs to the M2 phenotype, which further enhances cancer cell migration and metastasis (*23*). To explore the role of THAP7-AS1-activated EGFR-ELK1 signaling in macrophage polarization, the gene expression levels of a typical M0 marker (CD10B), M1 markers (NOS1), and M2 markers (CD206, CD163, TGFB, IL-4, IL-10, and ARG1) were investigated in THP-1 (human myeloid leukemia mononuclear cells) co-cultured with BC cells. Compared to the control group, the THP-1 co-cultured with THAP7-AS1-overexpressed BC cells showed remarkably higher expression of CD206, CD163, TGFB, IL-4, IL-10 and ARG1 and lower expression of NOS1, illustrating a predominant M2 phenotype (Figure 6G-H). By contrast, THP-1 co-cultured with THAP7-AS1-deleted BC cells showed notably decreased CD206, CD163, TGFB, IL-4, IL-10, and ARG1 and increased NOS1 (Figure 6I and Supplementary Figure 4K), indicating a distinct M1 phenotype. Flow cytometry analysis and western blot assay also indicated that the level of CD206 notably increased after THP-1 was co-cultured with THAP7-AS1-overexpressing BC cells (Figures 6J-L). These findings suggest that THAP7-AS1 increased the differentiation of M2 macrophages and decreased the differentiation of M1 macrophages.

M2 TAMs play a positive role in the enhancement of BC progression.

PMA (phorbol myristate acetate) has been shown to induce THP-1 cells differentiating into M2 TAMs (*24*). As shown in Figures 6M-N, cell morphology and the flow cytometry analysis suggest that PMA could induce the differentiation of THP-1 cells into M2 TAMs. Cell morphology and migration assays were then performed to explore the biological functions of M2 TAMs on BC cells, which were treated with the culture supernatants of TAMs. The results revealed that the BC cells showed epithelial-mesenchymal transformation and increased cell migration abilities when incubated with culture supernatants from TAMs (Figures 6O-P), which were concordant with the findings of previous reports indicating that TAMs play an active role in promoting the tumor cell invasion in human cancers(*25*). Next, the expression of CD163 (M2 markers) was examined by IHC in tumor xenografts. Figure 1M shows that there were less CD163+ cells in the THAP7-AS1 knockdown group compared with the control group.

Additionally, the gene expression of typical M1 markers (NOS1) and M2 markers (CD206, CD163, TGFB, IL-4, IL-10, and ARG1) was assessed. The expression of CD206, CD163, TGFB, IL-4, IL-10, and ARG1 significantly decreased in the THAP7-AS1 knockdown group (Figure 6Q), which coincided with the above results, indicating that tumor invasion abilities decreased in the THAP7-AS1 knockdown group partly due to the inhibition of M2 macrophage polarization. Therefore, these findings suggest that M2 TAMs play a positive role in the enhancement of BC progression.

M2 TAM upregulates THAP7-AS1 expression via IL-10/CEBP-β-dependent P300 expression in BC

We found that TAM not only promotes breast cancer progression, but also enhances THAP7-AS1 expression (Figures 7A-B). To determine whether TAM could mediate P300/c-MYC/c-JUN-induced THAP7-AS1 expression, we detected the levels of P300, c-MYC, and c-JUN in both BC cells with culture supernatants from TAMs. The results revealed that TAM increased the level of P300, but not c-MYC and c-JUN (Figures 7A-B). To confirm the effect of P300 on mediating TAM induced THAP7-AS1 upregulation, both BC cells were transfected with si-P300. The results showed that TAM-induced THAP7-AS1 upregulation was blocked by knocking down P300 (Figures 7C-D), suggesting that the P300 is critical in mediating TAM-induced THAP7-AS1.ChIP assays indicated that TAM directly enhances P300 and H3K27ac-binding abilities onto the THAP7-AS1 promoter (Figures 7E-H). M2 TAMs abundantly secrete cytokines [e.g., epidermal growth factor (EGF), FGF, IL-6, and IL-10], which are associated with tumor progression in many types of tumors, including breast cancer (*26-29*). Next, we performed Gene Expression Profiling Interactive Analysis (GEPIA) in BC from TCGA based on RNA-seq data, which demonstrate that EGF, FGF2, and IL-10 expression rather than IL-6 is positively correlated with P300 expression (Supplementary Figures 5A-D). To investigate the effect of EGF, FGF2 and IL-10 on P300 expression, we treated both BC cells with recombinant(r) EGF, rFGF2 and rIL-10. We found that rIL-10, rather than rEGF or rFGF2, increased P300 and THAP7-AS1 expression in both BC cells (Figures 7I-J). ELISA demonstrated that IL-10 concentrations in the TAMs supernatants markedly increased (Figure 7K). In addition, P300 knockdown inhibited rIL-10-induced THAP7-AS1 expression (Figures 7L-M), which suggests that rIL-10 increases THAP7-AS1 expression via P300. To investigate whether IL-10 transcriptionally upregulates P300 expression BC, we generated luciferase constructs containing the fragment -2,000 bp to 0 bp upstream of the TSS of the P300 promoter sequences. Luciferase assays showed higher promoter activities of PGL3-2,000/0 compared to that of pGL3-basic (Figures 7N-O and supplementary Figure 5E). Moreover, rIL-10 increased PGL3-2000/0 promoter activity in 293T cells (Figure 7P). Next, ALGGEN program was used to predict the transcription factor-binding site region. Three putative binding sites, including c-MYB, YY1, and CEBP-β-binding sites, were identified. To explore their roles in regulating P300 transcription, luciferase, RT-qPCR, and ChIP assays were performed. The results indicated that CEBP-β directly binds to its promoter and regulates THAP7-AS1 transcription (Figures 7Q-S and supplementary Figure 5F). Additionally, IL-10 activates distinct JAK2-STAT3 pathways to influence nuclear transcriptional events, resulting in the upregulation of transcription factor C/EBPβ (*30-32*). We also confirmed that CEBP-β expression was upregulated in TAM- and rIL-10-treated BC cells (Figures 7T-U). Additionally, we found that M2 TAM promoted the expression of the key molecules in EGFR signaling

(supplementary Figure 5G). Collectively, M2 TAMs induce THAP7-AS1 upregulation and activate EGFR signaling via IL-10/CEBP-β-dependent P300 expression in BC.

Discussion

In our previous study, we identified a novel lncRNA THAP7-AS1, which is significantly upregulated in cancer tissues compared with normal tissues by lncRNA microarray screening and tissue sample validation. These findings indicate a tumor- promoter role for THAP7-AS1. However, the potential functions and mechanistic details for THAP7-AS1 in human BC still remain unclear. Here, we found that THAP7-AS1 is remarkably upregulated in BC tissues, especially in lymph node metastatic BC. Additionally, THAP7-AS1 promotes BC cell invasion and metastasis *in vitro* and *in vivo*. These findings suggest that THAP7-AS1 acts as an oncogene in BC, and its overexpression leads to BC tumorigenesis and progression.

Notably, accumulating evidence has demonstrated that lncRNAs play a wide range of roles in the pathogenesis of multiple diseases through diverse mechanisms of downstream gene modulation such as epigenetic, post-transcriptional, and transcriptional regulation. Herein, we found that instead of regulating neighboring gene THAP7, THAP7-AS1 activates EGFR expression through recruitment of the SWI/SNF complex and subsequently triggers EGFR signaling to promote tumor progression of BC cells. The SWI/SNF chromatin remodelers complex are composed of approximately 15 protein subunits containing one of two catalytic ATPase subunits, namely, SMARCA4 (also known as BRG1) or SMARCA2 (also known as BRM) and several core components such as SMARCB1 (also known as SNF5), BAF170, and BAF155 (33). The SWI/SNF complex mobilizes nucleosomes and remodels chromatin to regulate gene expression using energy derived from ATP hydrolysis (34), indicating its key roles in regulating gene expression at the transcriptional level. Here, we found that THAP7-AS1 can recruit the SWI/SNF complex to trigger EGFR expression and activate EGFR-ELK1 signaling, resulting in the expression and secretion of IL-4 and metastasis of BC. The status of chromatin structure, how DNA is packaged in eukaryotic cells, has a major impact on the activation/suppression of gene expression. The best-characterized chromatin-altering mechanism is histone acetylation, which is catalyzed by histone acetyltransferase (HAT) (35). Here, we showed that THAP7-AS1 expression was significantly enhanced in TSA-treated BC cell. P300 possesses intrinsic HAT activity, which regulates the transcription of specific genes by functioning as a coactivator in SP1-, Ets-, AP-1-, NF-AT-, and GATA-mediated transcription (36). In the present study, we found that P300 acts synergistically with c-MYC to activate the THAP7-AS1 gene.

Mounting evidence has shown that TAMs are correlated with tumor growth, invasion, metastasis, and angiogenesis in response to various microenvironmental from cancer and stromal cells (22). Studies have shown that IL-4 is a potential tumor activator and promotes M2 macrophage activation. We found that THAP7-AS1-induced IL-4 expression promotes M2 polarization of TAMs, and TAMs upregulate THAP7-AS1 levels via IL-10/CEBP-β-dependent P300 expression in BC. Our studies demonstrated that TAMs and cancer cells can form positive feedback loops to maintain high THAP7-AS1 levels to promote BC progression.

The present study has revealed a new biological role for THAP7-AS1 in promoting the BC metastasis via activation of TAMs. THAP7-AS1 recruits the SWI/SNF complex to upregulate EGFR expression, and then activates EGFR-ELK1 signaling-mediated IL-4 expression, which results in the polarization of TAMs towards the M2 phenotype in BC. Importantly, IL-10 secreted by TAMs activates the CEBP-β-induced P300 expression. In addition, P300, which interacts with c-MYC, could activate THAP7-AS1 transcription to form a positive feedback loop to maintain BC progression (Fig. 7V). Collectively, we have revealed a novel role for THAP7-AS1 in the regulation of crosstalk between TAM and tumor cells in BC, thereby improving our understanding of BC progression. In addition, this study presents novel therapeutic targets for BC treatment.

Declarations

Competing interests Statement

The authors declare no competing interests.

Author contributions Statement

P Gao and H-T Liu performed the conception and design of this manuscript. H-T Liu, Z-X Gao, G-H Zhang, X-Y Guo, X-C Zhou, R-N Zhao, S Liu, W-J Zhu, C-Z Zhao and X Wang collected clinical tumor samples. F-Z Zhang and H Wan performed RNA and plasmid extraction. H-T Liu and P Gao performed data analysis and interpretation. H-T Liu and P Gao performed the manuscript writing. All authors were involved in writing the paper and had final approval of the final manuscript.

Ethics Statement

Fresh BC tissues and nontumorous breast tissues were collected from the Qilu Hospital of Shandong University, which was approved by the Research Ethics Committee of Shandong University. All participants have informed consent and their privacy has been fully protected. All of the animal experiments were conducted according to the Guidelines for Animal Health and Use (Ministry of Science and Technology, China, 2006). Animal experiments were approved by the Committee for Animal Protection of Shandong University.

Funding Statement

This study was supported by the National Natural Science Foundation of China (Grant No. 81872362, 82072665 and 82103564) and Natural Science Foundation of Shandong Province (Grant No. ZR2020QH223).

Acknowledgments:

We thank LetPub (www.letpub.com) for its linguistic assistance during the preparation of this manuscript.

Data Availability Statement

All data generated or analyzed during this study are included in this published article and its supplementary information files. Microarray data were deposited in NCBI Gene Expression Omnibus (GEO, GSE 150539 and GSE160685).

References

1. J. E. Bradner, D. Hnisz, R. A. Young, Transcriptional Addiction in Cancer. Cell **168**, 629–643 (2017).
2. H. Dong *et al.*, Activation of LncRNA TINCR by H3K27 acetylation promotes Trastuzumab resistance and epithelial-mesenchymal transition by targeting MicroRNA-125b in breast Cancer. Molecular cancer **18**, 3 (2019).
3. K. D. Miller *et al.*, Cancer treatment and survivorship statistics, 2019. CA: a cancer journal for clinicians **69**, 363–385 (2019).
4. L. Hui, Y. Chen, Tumor microenvironment: Sanctuary of the devil. Cancer letters **368**, 7–13 (2015).
5. T. Chanmee, P. Ontong, K. Konno, N. Itano, Tumor-associated macrophages as major players in the tumor microenvironment. Cancers **6**, 1670–1690 (2014).
6. M. De Palma, C. E. Lewis, Macrophage regulation of tumor responses to anticancer therapies. Cancer cell **23**, 277–286 (2013).
7. A. L. Welm *et al.*, The macrophage-stimulating protein pathway promotes metastasis in a mouse model for breast cancer and predicts poor prognosis in humans. Proceedings of the National Academy of Sciences of the United States of America **104**, 7570–7575 (2007).
8. J. Chen *et al.*, CCL18 from tumor-associated macrophages promotes breast cancer metastasis via PITPNM3. Cancer Cell **19**, 541–555 (2011).
9. X. Zhang, T. T. Ho, Computational Analysis of lncRNA Function in Cancer. Methods in molecular biology **1878**, 139–155 (2019).
10. L. Qu *et al.*, Exosome-Transmitted lncARSR Promotes Sunitinib Resistance in Renal Cancer by Acting as a Competing Endogenous RNA. Cancer Cell **29**, 653–668 (2016).
11. P. Zhu *et al.*, lnc-beta-Catm elicits EZH2-dependent beta-catenin stabilization and sustains liver CSC self-renewal. Nat Struct Mol Biol **23**, 631–639 (2016).
12. J. Zheng *et al.*, Pancreatic cancer risk variant in LINC00673 creates a miR-1231 binding site and interferes with PTPN11 degradation. Nat Genet **48**, 747–757 (2016).
13. M. C. Tsai *et al.*, Long noncoding RNA as modular scaffold of histone modification complexes. Science **329**, 689–693 (2010).
14. H. T. Liu, S. Liu, L. Liu, R. R. Ma, P. Gao, EGR1-Mediated Transcription of lncRNA-HNF1A-AS1 Promotes Cell-Cycle Progression in Gastric Cancer. Cancer Res **78**, 5877–5890 (2018).
15. W. X. Peng, P. Koirala, Y. Y. Mo, LncRNA-mediated regulation of cell signaling in cancer. Oncogene **36**, 5661–5667 (2017).

16. G. M. Euskirchen *et al.*, Diverse roles and interactions of the SWI/SNF chromatin remodeling complex revealed using global approaches. PLoS Genet **7**, e1002008 (2011).
17. T. L. Hilton, Y. Li, E. L. Dunphy, E. H. Wang, TAF1 histone acetyltransferase activity in Sp1 activation of the cyclin D1 promoter. Molecular and cellular biology **25**, 4321–4332 (2005).
18. T. Narita, B. T. Weinert, C. Choudhary, Functions and mechanisms of non-histone protein acetylation. Nat Rev Mol Cell Biol **20**, 156–174 (2019).
19. H. M. Chan, N. B. La Thangue, p300/CBP proteins: HATs for transcriptional bridges and scaffolds. Journal of cell science **114**, 2363–2373 (2001).
20. D. A. Bose *et al.*, RNA Binding to CBP Stimulates Histone Acetylation and Transcription. Cell **168**, 135–149 e122 (2017).
21. F. Tie *et al.*, CBP-mediated acetylation of histone H3 lysine 27 antagonizes Drosophila Polycomb silencing. Development **136**, 3131–3141 (2009).
22. Y. Cheng *et al.*, PKN2 in colon cancer cells inhibits M2 phenotype polarization of tumor-associated macrophages via regulating DUSP6-Erk1/2 pathway. Mol Cancer **17**, 13 (2018).
23. Y. Zhang, W. Sime, M. Juhas, A. Sjolander, Crosstalk between colon cancer cells and macrophages via inflammatory mediators and CD47 promotes tumour cell migration. European journal of cancer **49**, 3320–3334 (2013).
24. F. Xu *et al.*, Astragaloside IV inhibits lung cancer progression and metastasis by modulating macrophage polarization through AMPK signaling. Journal of experimental & clinical cancer research: CR **37**, 207 (2018).
25. S. Su *et al.*, A positive feedback loop between mesenchymal-like cancer cells and macrophages is essential to breast cancer metastasis. Cancer Cell **25**, 605–620 (2014).
26. S. Wan *et al.*, Tumor-associated macrophages produce interleukin 6 and signal via STAT3 to promote expansion of human hepatocellular carcinoma stem cells. Gastroenterology **147**, 1393–1404 (2014).
27. H. Jeong *et al.*, Tumor-Associated Macrophages Enhance Tumor Hypoxia and Aerobic Glycolysis. Cancer Res **79**, 795–806 (2019).
28. M. Yin *et al.*, Tumor-associated macrophages drive spheroid formation during early transcoelomic metastasis of ovarian cancer. J Clin Invest **126**, 4157–4173 (2016).
29. F. Chen *et al.*, Extracellular vesicle-packaged HIF-1alpha-stabilizing lncRNA from tumour-associated macrophages regulates aerobic glycolysis of breast cancer cells. Nat Cell Biol **21**, 498–510 (2019).
30. Y. Zhu, Z. Liu, Y. P. Peng, Y. H. Qiu, Interleukin-10 inhibits neuroinflammation-mediated apoptosis of ventral mesencephalic neurons via JAK-STAT3 pathway. Int Immunopharmacol **50**, 353–360 (2017).
31. Z. H. Wang *et al.*, Deficiency in BDNF/TrkB Neurotrophic Activity Stimulates delta-Secretase by Upregulating C/EBPbeta in Alzheimer's Disease. *Cell Rep* **28**, 655–669 e655 (2019).
32. H. Zhang *et al.*, STAT3 controls myeloid progenitor growth during emergency granulopoiesis. Blood **116**, 2462–2471 (2010).

33. B. H. Alver *et al.*, The SWI/SNF chromatin remodelling complex is required for maintenance of lineage specific enhancers. Nat Commun **8**, 14648 (2017).
34. M. Y. Tolstorukov *et al.*, Swi/Snf chromatin remodeling/tumor suppressor complex establishes nucleosome occupancy at target promoters. Proc Natl Acad Sci U S A **110**, 10165–10170 (2013).
35. E. Ortega *et al.*, Transcription factor dimerization activates the p300 acetyltransferase. Nature **562**, 538–544 (2018).
36. C. Liu, J. Lu, J. Tan, L. Li, B. Huang, Human interleukin-5 expression is synergistically regulated by histone acetyltransferase CBP/p300 and transcription factors C/EBP, NF-AT and AP-1. Cytokine **27**, 93–100 (2004).

Figures

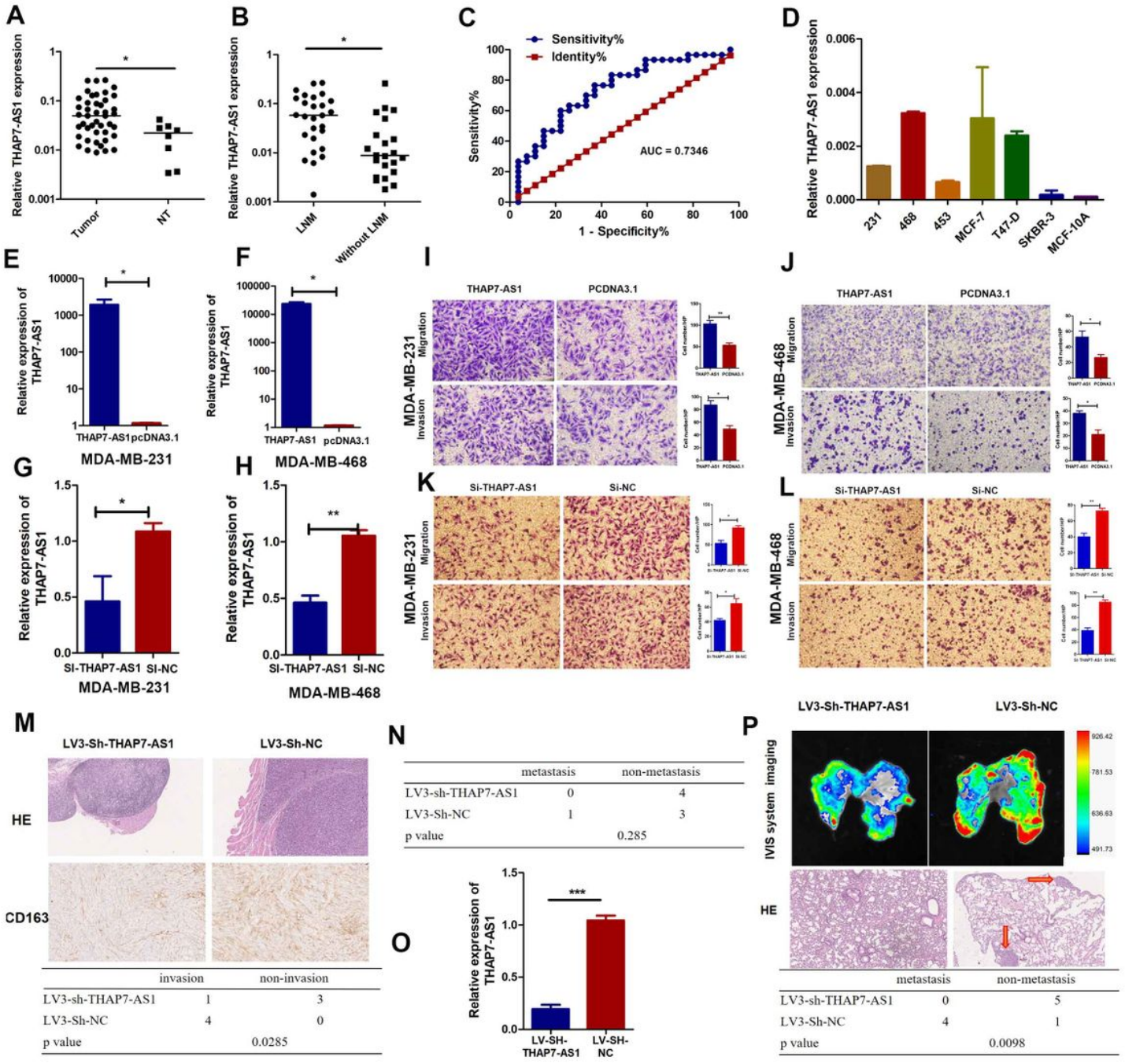

	metastasis	non-metastasis
LV3-sh-THAP7-AS1	0	4
LV3-Sh-NC	1	3
p value	0.285	

	invasion	non-invasion
LV3-sh-THAP7-AS1	1	3
LV3-Sh-NC	4	0
p value	0.0285	

	metastasis	non-metastasis
LV3-sh-THAP7-AS1	0	5
LV3-Sh-NC	4	1
p value	0.0098	

Figure 1

THAP7-AS1 is up-regulated in human BC tissues and enhances BC cells' metastatic ability

(A)THAP7-AS1 expression in 44 BC tumors and 8 non-tumor tissues using qRT-PCR was detected. (B)THAP7-AS1 expression was remarkably higher in the lymph node metastatic (LNM) BC than without LNM BC tissues. (C) A receiver operating characteristic (ROC) curve was performed to evaluate whether THAP7-AS1 expression could be used to distinguish patients with or without LNM. (D)THAP7-AS1 expression level in a panel of human BC cell lines and nontumorous mammary epithelial cells MCF10A was detected. (E-F) The overexpression efficiency of THAP7-AS1 in MDA-MB-231 (E) and MDA-MB-468 cells(F) was examined. (G-H) The knockdown efficiency of THAP7-AS1 in MDA-MB-231 (G) and MDA-MB-

468 cells (H) was measured. (I-J) MDA-MB-231 (I) and MDA-MB-468 cells (J) were transfected with the indicated constructs, and migration and invasion abilities were determined using Transwell assays. (K-L) MDA-MB-231(K) and MDA-MB-468 cells (L) were transfected with the SI-THAP7-AS1 and SI-NC, and migration and invasion abilities were observed using Transwell assays. (M-N) Less local infiltration (M; top), a lower positivity rate in CD-206 (M; middle) and metastatic colonies (N) in the lung were observed xenograft tumor models in nude mice using MDA-MB-231 cells with stable transfection of LV3-sh-THAP7-AS1 or LV3-sh-NC. (O) THAP7-AS1 expression was detected in LV3-sh-THAP7-AS1 group and LV3-sh-NC group. (P) The number of metastatic nodules were reduced in in nude mice received tail vein administration of ectopic knockdown of THAP7-AS1 compared with the control group.

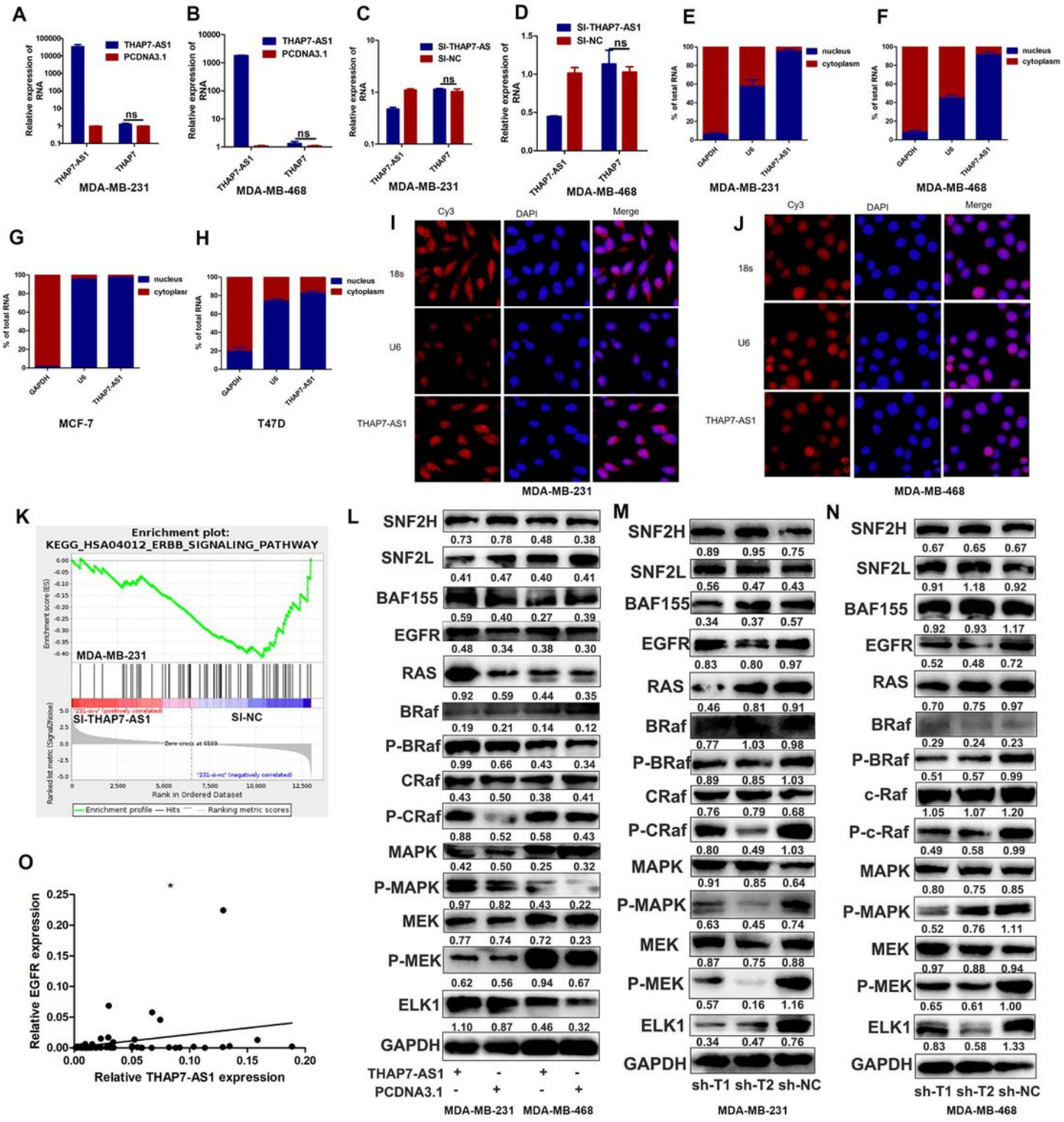

Figure 2

THAP7-AS1 activate EGFR Signaling pathway

(A-B) THAP7-AS1 and THAP7 expression were detected in THAP7-AS1 overexpressed MDA-MB-231(A) and MDA-MB-468 cells(B).(C-D) Relative expression of THAP7-AS1 and THAP7 in MDA-MB-231(C) and MDA-MB-468 cells (D) after transfected with SI-THAP7-AS1 compared with controls.(E-H)

Nuclear/cytoplasm fractionation assay was performed to observe the cellular location of THAP7-AS1 in MDA-MB-231(E), MDA-MB-468 cells (F), MCF-7(G) and T47D (H).(I-J) RNA FISH assay was used to detect the cellular location of THAP7-AS1 in MDA-MB-231(I), MDA-MB-468 cells (J). (K) GSEA indicated that ERBB (EGFR) related gene signatures in an RNA-seq data set were enriched for downregulation upon THAP7-AS1 knockdown. (L) Western blotting assays showed that THAP7-AS1 overexpression significantly upregulated the expression of some major EGFR signaling targets, including EGFR, RRAS and ELK1, phosphorylation of BRAF, CRAF, MAPK and ERK in MDA-MB-231 and MDA-MB-468 cells. (M-N) THAP7-AS1 depletion deceased the expression of EGFR and major EGFR targets. (O) A significant positive correlation was found between the levels of THAP7-AS1 and EGFR in BC tissues.

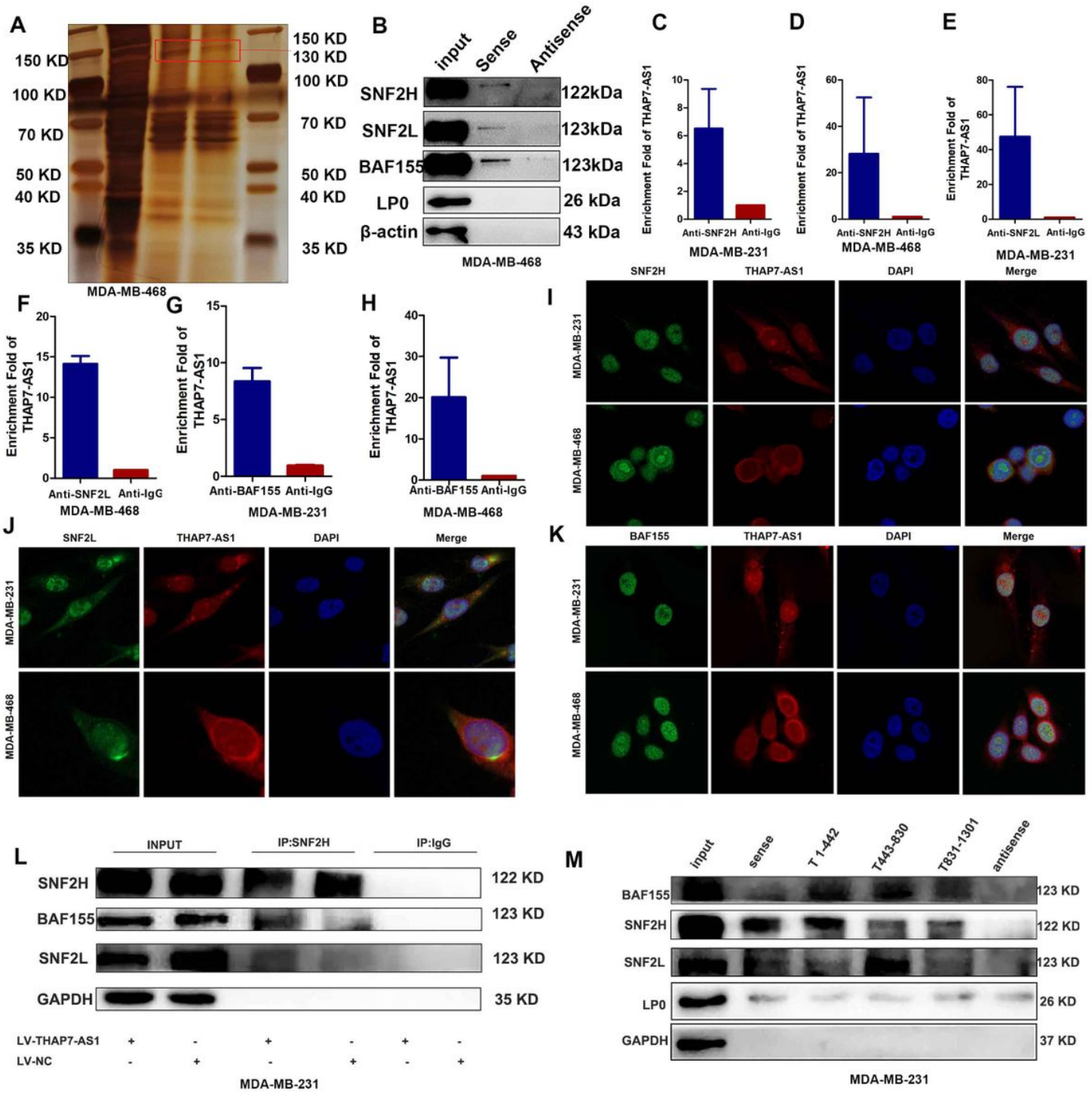

Figure 3

THAP7-AS1 directly binds with SWI/SNF Complex

(A) Proteins that specially interacted with the THAP7-AS1 were identified by combining RNA-pulldown, silver staining and mass spectrometry in MDA-MB-468 cells. (B) RNA pull-down assay was confirmed the interaction between the THAP7-AS1 and three SWI/SNF components in MDA-MB-468 cells. (C-H) RNA immunoprecipitation was further confirmed the interaction between the three SWI/SNF components and THAP7-AS1. (I-K) Confocal micrographs indicated that THAP7-AS1 colocalized with SNF2H (I), SNF2L(J) and BAF155(K) in the nuclei of both BC cells. (L) Overexpression of THAP7-AS1 promoted the interaction between SNF2H and SNF2L and BAF155. (M) Domain mapping suggested that we observed that segment 1 (–) of THAP7-AS1 interacted with SNF2H, segment 2 (–) combined with SNF2L, whereas segment 3 (–) bound to BAF155 in MDA-MB-468 cells.

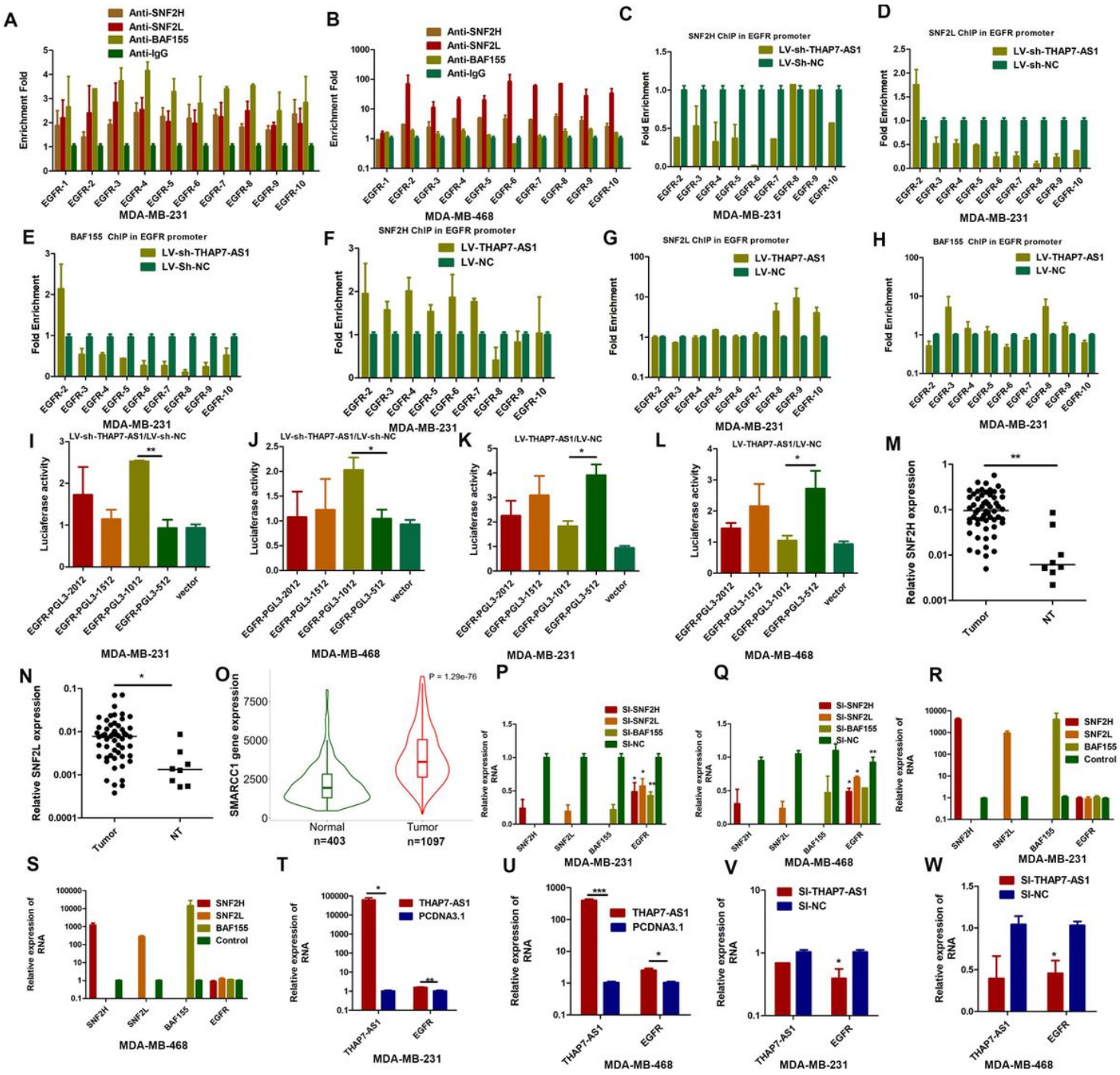

Figure 4

THAP7-AS1 triggers EGFR expression through recruitment of the SWI/SNF complex to activate EGFR signaling

(A-B) The EGFR promoter is sufficient for the binding of SNF2H, SNF2L and BAF170 by ChIP-quantitative PCR analysis in MDA-MB-231 cells (A) and MDA-MB-468 cells (B). (C-E) THAP7-AS1 depletion decreased the binding capacity of SNF2H, SNF2L and BAF155 with EGFR promoter. (F-H) The interaction of SNF2H, SNF2L and BAF155 with EGFR promoter region can be enhanced by THAP7-AS1 upregulation. (I-L) Different loci of EGFR promoter were constructed into pGL3 vector and subjected to luciferase reporter

assays in THAP7-AS1-silenced and overexpressed both BC cells. (M-N). SNF2H(M) and SNF2L(N) were highly expressed in BC tumors compared with non-tumorous breast tissues. (O) BAF155 were remarkably upregulated in BC tissues from the TCGA data. (P-S) The expression of SNF2H, SNF2L, BAF155 and EGFR were detected in SNF2H, SNF2L, BAF155 respectively silenced and overexpressed BC cells. (T-W) The expression of THAP7-AS1 and EGFR were detected in THAP7-AS1 upregulated and silenced BC cells.

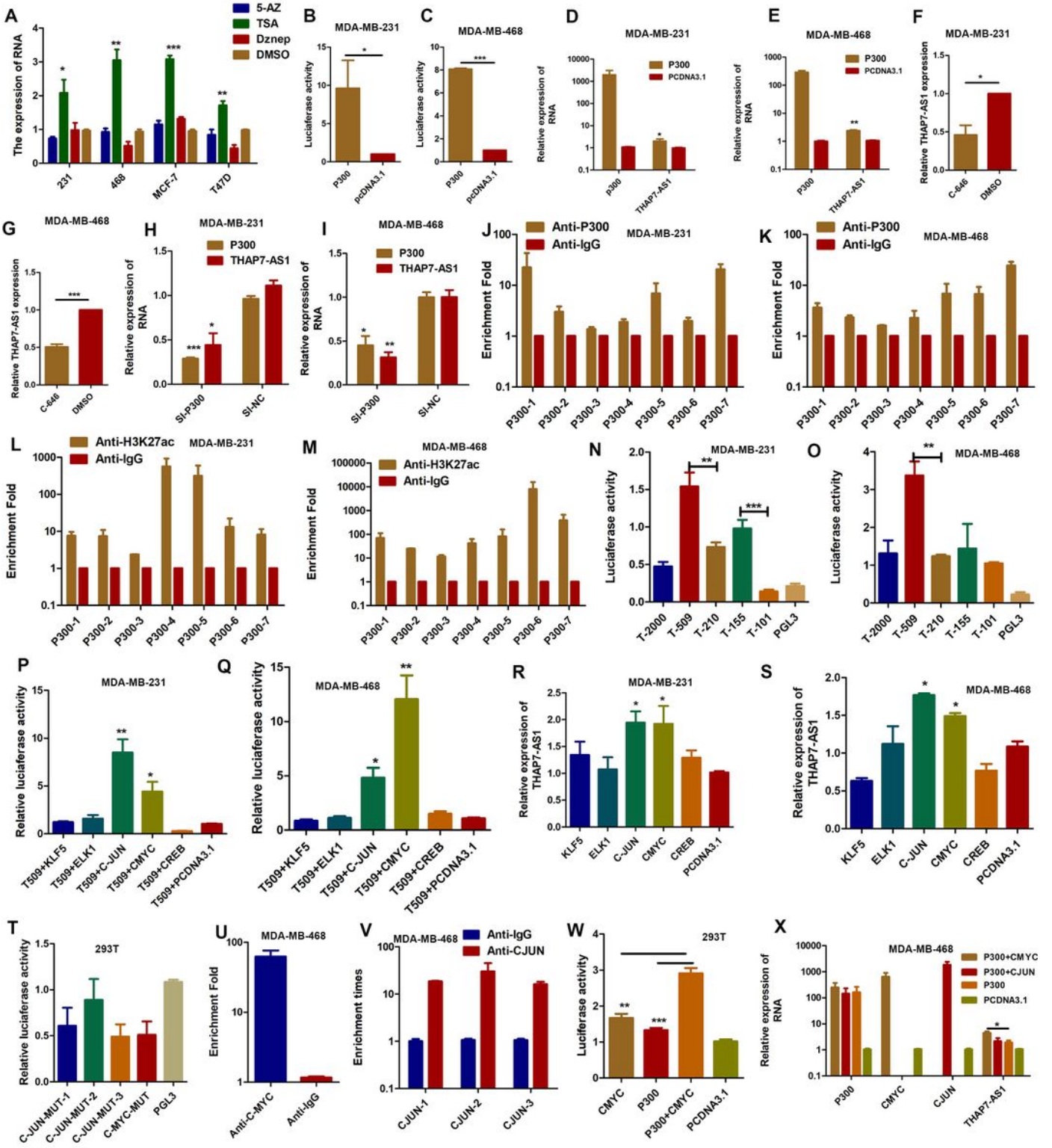

Figure 5

P300 and c-MYC synergistically activates THAP7-AS1 transcription

(A) The expression of THAP7-AS1 was detected in four BC cells treated with 5-Azacytidine (5-AZ, demethylating agent), trichostatin A (TSA; histone deacetylase inhibitor) and 3-deazaneplanocin A (Dznep, histone methyltransferase EZH2 inhibitor). (B-C) Luciferase activity assay revealed that P300 was able to promote the transcriptional activity of THAP7-AS1 promoter in BC cells. (D-E) The expression of THAP7-AS1 and P300 were detected in P300-overexpressed BC cells. (F-G) The expression of THAP7-AS1 was observed in BC cells treated with C-646 (histone acetyltransferase (HAT)-P300 inhibitors). (H-I) The expression of THAP7-AS1 and P300 were measured in P300-silenced BC cells. (J-M) ChIP-qPCR analysis showed higher fold enrichment of promoter amplicons of P300 and H3K27me3 in anti-P300 and anti-H3K27me3 antibody group than that of IgG group in BC cells. (N-O) Transcriptional activity analysis of the potential THAP7-AS1 promoter fragments (PGL3-2,000/ -509/ -210/ -155/-101) in BC cells. (P-Q) Luciferase activity assay demonstrated that c-JUN and c-MYC observably enhanced promoter activities of pGL3−509/0. (R-S) RT-qPCR assay showed c-JUN and c-MYC increased the expression level of THAP7-AS1 in BC cells. (T) Luciferase activity of the THAP7-AS1 promoter was reduced when the three c-JUN and one c-MYC presumed THAP7-AS1 binding sites were respectively mutated in 293T cells. (U-V) ChIP-qPCR analysis indicated higher fold enrichment of promoter regions of c-MYC and c-JUN in anti-c-MYC (U) and anti-c-JUN antibody (V) group than that of IgG group in MDA-MB-468 cells. (W) Luciferase activity indicated that P300 was worked synergistically with c-MYC, rather than c-JUN, to increase THAP7-AS1 promoter activity. (X) RT-qPCR assay showed that P300 was worked synergistically with c-MYC to increase THAP7-AS1 expression.

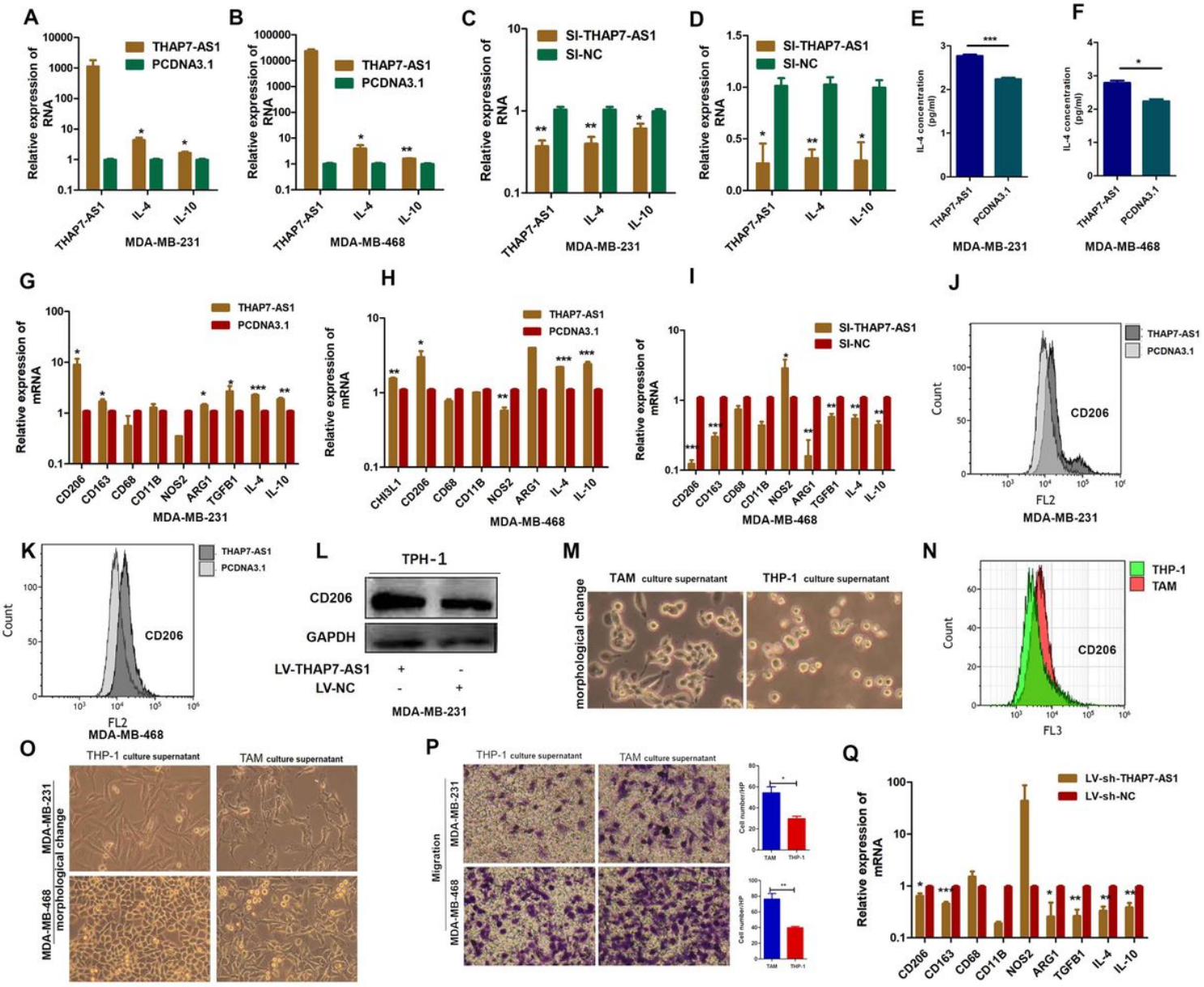

Figure 6

THAP7-AS1 promote M2 macrophage polarization

(A-D)The mRNA level of IL-4 and IL-10 was detected in THAP7-AS1-overexpressed and silenced BC cells. (E-F) ELISA assay showed significantly increased IL-4 levels were observed in THAP7-AS1 overexpressed BC cells. (G-I) The gene expression of typical M0 marker (CD10B), M1 markers (NOS1) and M2 markers (CD206, CD163, TGFB, IL-4, IL-10 and ARG1) was investigated in THP-1 (human myeloid leukemia mononuclear cells) co-cultured with THAP7-AS1 overexpressed (G-H) or silenced (I) BC cells. (J-L) The flow cytometry analysis (J-K) and Western Blot assay (L) indicated that the level of CD206 were notably increased after the THP-1 co-cultured with THAP7-AS1-overexpressed BC cells. (M-N) cell morphology (M) and the flow cytometry analysis (N) suggested that PMA could induce THP-1 cells differentiating into M2 TAMs. (O-P) Cell morphology (O) and migration assay (P) was performed to explore the biological functions of M2 TAMs on BC cells. (Q) The gene expression of typical M1 markers (NOS1) and M2

markers (CD206, CD163, TGFB, IL-4, IL-10 and ARG1) was determined in THAP7-AS1 knockdown and group tumor xenograft.

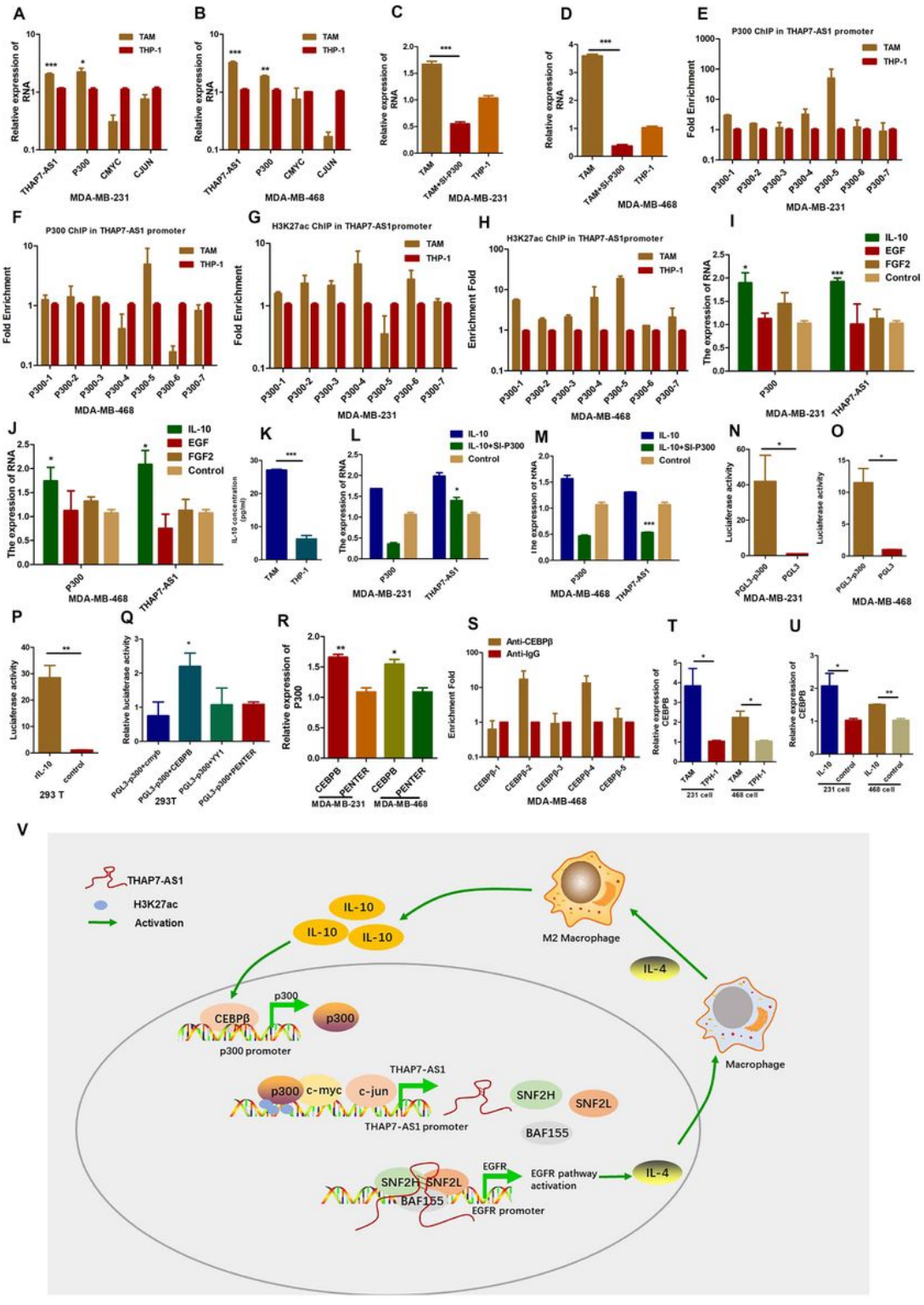

Figure 7

TAM upregulates THAP7-AS1 expression via IL-10/ CEBP-β -dependent P300 expression in BC

(A-B) The expression of THAP7-AS1, P300, c-MYC and c-JUN was detected in both BC cells with culture supernatants from TAMs and THP-1. (C-D) RT-qPCR assay revealed that TAM-induced THAP7-AS1 overexpression was blocked by knockdown P300. (E-H) ChIP-qPCR analysis showed TAM directly enhanced P300 and H3K27ac-binding abilities on THAP7-AS1 promoter in anti-P300 and anti-H3K27me3 antibody group than that of IgG group in BC cells. (I-J) The expression of P300 and THAP7-AS1 was detected in both BC cells treated with recombinant(r) EGF, rFGF2 and rIL-10. (K) ELISA assay was performed to determine the IL-10 concentration in the TAMs and THP-1 supernatants. (L-M) rIL-10 increased P300 and THAP7-AS1 expression in both BC cells, whereas P300 knockdown in BC cells inhibited rIL-10-induced THAP7-AS1 expression. (N-O) The promoter activities of PGL3-2000/0 led to increase in luciferase activity compared to that of pGL3-basic. (P) Luciferase assays demonstrated that PGL3-2000/0 promoter activity increased in rIL-10 induced 293T cells. (Q) c-MYB, YY1 and CEBP-β remarkably increased the promoter activities of pGL3-2000/0. (R) RT-qPCR assay suggested that CEBP-β increased the expression of P300. (S) ChIP-qPCR analysis showed higher fold enrichment of promoter regions of CEBP-β in anti-CEBP-β antibody group than that of IgG group in BC cells. (U) CEBP-β expression was upregulated in TAM- and rIL-10- treated BC cells. (V) Proposed functional action of THAP7-AS1-SWI/SNF complex in modulating BC progression. THAP7-AS1 recruits the SWI/SNF complex to trigger EGFR expression, resulting in activation of EGFR-ELK1 signaling for promoting BC metastasis. THAP7-AS1 increased the polarization of TAMs towards the M2 phenotype by promoting ELK1-mediated IL-4 expression in BC cells. Importantly, IL-10 secreted by TAMs may activate the CEBP-β-induced P300 expression. Furthermore, we also found that P300, cooperated with transcription factor (TF) c-MYC could activate THAP7-AS1 transcription.

Supplementary Files

This is a list of supplementary files associated with this preprint. Click to download.

- SupplementaryFigureandFigureLegend.docx
- SupplementaryTable14.docx